XIV SYMPOSIUM OF SPECIALISTS IN ELECTRIC OPERATIONAL AND EXPANSION PLANNING

SEPTEMBER 30TH THRU OCTOBER 3RD OF 2018 / RECIFE / PE /BRASIL

Use of disjunctive constraints to represent risk aversion policies

F.G. CABRAL[1,2], B. F.P. COSTA[2], J.P. COSTA[1]
[1]ONS – Operador Nacional do Sistema Elétrico
[2]UFRJ – Universidade Federal do Rio de Janeiro
Brazil

SUMMARY

In this article, we propose a methodology to represent the operational procedures of the Brazilian power system focused on the security of the electric energy supply. The approach takes into account the fundamental difference between conservation laws (physical limits) and operational rules. The former are hard constraints while the latter are soft constraints that must be imposed if feasible, but if not, a weaker alternative must be considered. For instance, hydraulic balance equations are hard constraints while minimum storage targets are soft constraints. A standard approach to deal with operational constraints in the power system planning resorts to artificial penalties. However, this approach often leads to decisions that are not always the aimed ones and also misrepresent the economical interpretation of total and marginal costs. The proposed methodology, using disjunctive programming, describes the feasible region of operation as a union of polyhedral sets. It does not make use of artificial prices and represents soft constraints more accurately than traditional penalty schemes. Under special circumstances, the polyhedra are ordered by cost, and thus exactly describe the ordering of the operational rules. The resulting formulation includes binary variables, and recent algorithmic advances in multistage mixed integer stochastic programming (SDDiP, proposed by Zou, Ahmed and Sun in 2016) make the solution of the model computationally tractable. We illustrate the consistency of this proposal with a case study considering a long-term operational planning problem of the Brazilian Interconnected Power System.

KEYWORDS

Operation planning, multistage stochastic programming, Stochastic Dual Dynamic *integer* Programming, risk aversion.

[1]e-mail: fcabral@ons.org.br; fone +55 21 3444 9641
ONS – Rua Júlio do Carmo, 251 - Cidade Nova, 20211-160 – Rio de Janeiro – RJ

XIV SYMPOSIUM OF SPECIALISTS IN ELECTRIC OPERATIONAL AND EXPANSION PLANNING

SEPTEMBER 30TH THRU OCTOBER 3RD OF 2018 / RECIFE / PE /BRASIL

1 Introduction

Physical constraints are generally given by bounds on the physical quantities, and conservation laws for mass, energy, and moment. We use equality and inequality constraints involving the corresponding quantities to model these laws and bounds, since they are *inviolable* relations and must be respected for any decision and initial state of the physical system. In many cases, such constraints can be modeled by linear equations, which induce convex feasible sets.

Operational constraints, on the other hand, follow rules that may be accommodated depending on the state of the system. One example of such rule has to do with operational security concerns related to low storage volumes of the reservoirs of a hydrothermal power system. One way to represent these concerns is to avoid low stored volumes, which can be attained by establishing a minimum energy storage level (v_{MinOp}) for the equivalent reservoir of the hydro system that, whenever the stored energy level falls below v_{MinOp}, imposes compulsory thermal generation.

Another example is given by Resolution 2081 issued by the National Water Agency (ANA) on December 4, 2017 [1], regarding the conditions for the operation of the São Francisco River Water System. This resolution establishes the operational rules for the outflow of the reservoirs of the system according to the storage level of Três Marias and Sobradinho reservoirs.

These and other operational rules can be set in the framework of “if-then” constraints that must be enabled or disabled as required. It is natural to use binary variables to model this “on-off” behavior, which can induce non-convex feasible sets. Yet, it may not be easy to obtain a description of such sets by trial and error. We propose the use of the Disjunctive Constraints technique [2, 3, and 4] that provides a general method of describing “if-then” rules in terms of union of polyhedra and are represented by 0-1 mixed integer linear constraints.

In sections 2 and 3 we present a general methodology to deal with this kind of constraints. In section 4 an example regarding security levels for the Brazilian Power System is presented and discussed.

2 Examples of operational constraints

In this section, we present two operational rules v_{MinOp} and ANA, and examine the process of transforming them into mathematical constraints to be incorporated in an optimization model. We follow the point of view of using “binary if-then rules”.

2.1 Minimum Operational Volume

The Minimum Operational Volume (v_{MinOp}) is a stored energy reference that is used as a signal of imminent risk of energy supply for the Brazilian Power System. Indeed, if the stored energy of any subsystem falls below the settled v_{MinOp}, then it is agreed that a minimum amount of thermal generation must be compulsorily dispatched.

At a given time *t*, we denote by $v_{\mathrm{MinOp},t}$ the vector corresponding to the minimum security energy level of each subsystem, by v_{t+1} the vector of stored energy at the end of time *t* (beginning of time *t*+1), by g_t the generation of each thermal plant during stage *t*, and by $\underline{G_t}$ the vector of security thermal dispatch of each thermal plant. We omit the subscript *t* of v_{MinOp} and $\underline{G}$ in the following text so as to not overload the notation. The constraints corresponding to the binary v_{MinOp} rules are:

$$v_{t+1} \geq (1 - z_g) v_{\text{MinOp}}$$
$$g_t \geq z_g \underline{G} \tag{1}$$
$$z_g \in \{0, 1\}$$

where z_g is a binary variable that indicates whether or not the final stored energy v_{t+1} is below the security level v_{MinOp}. If z_g equals 1, the thermal generation lower bound is raised to a level $\underline{G}$, whether if z_g equals 0, there is no constraint on minimum compulsory thermal generation. The resulting feasible set for the variables (v_{t+1}, g_t) is depicted in Figure 1.

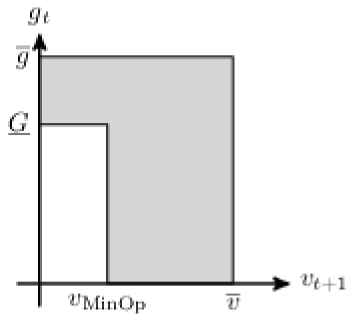

FIGURE 1: Binary v_{MinOp}.

Note that, if we used one binary variable for each subsystem, we would have the slightly different rule that, if the stored energy of a subsystem falls below the corresponding target, just a group of thermal plants is dispatched, instead of all of them.

2.2 Minimum Outflow

The rule regarding the minimum reservoir outflow is more involved. The objective of this rule is to ensure a minimum reservoir outflow to meet the multiple uses of water. However, in shortage situations, the National Water Agency (ANA) [1] determines smaller outflow values to guarantee the continuity of water supply for essential activities. Figure 2 illustrates the feasible set corresponding to the ANA rules, translated into equivalent energy for the optimization model.

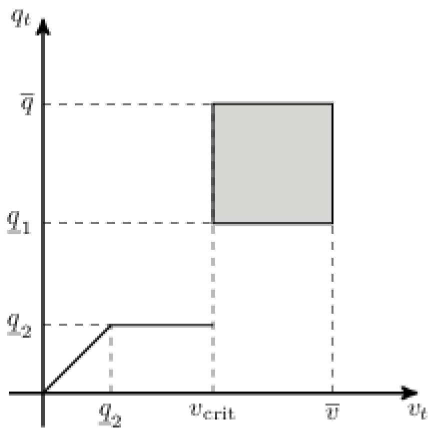

FIGURE 2: Minimum outflow operational rule.

The minimum energy outflow in normal circumstances is $\underline{q}_1$. $\underline{q}_2$ is a smaller outflow value for shortage situations, and v_{crit} is the critical energy storage below which we consider an outflow of $\underline{q}_2$, instead of $\underline{q}_1$. Note that for stored values v_t above v_{crit}, the parameter $\underline{q}_1$ is just a lower bound for the outflow q_t, but for stored values between $\underline{q}_2$ and v_{crit} the corresponding outflow is exactly $\underline{q}_2$. For stored volumes below $\underline{q}_2$ the outflow is the remaining stored volume v_t, that is, the decision is to empty the reservoir. In this case, it is difficult to find a set of constraints using binary variables that represents the rules depicted in Figure 2 by trial and error. Section 3 presents a systematic approach for modeling non-convex feasible sets using binary variables.

3 Disjunctive Constraints: a general modeling technique

Disjunctive Programming (DP) was developed by Balas [2, 3, and 4]. A disjunction is a set of constraints of which at least one must be satisfied. In our setting, this corresponds to different elementary feasible regions, and we demand that our decision variables belong to at least one of them.

In the linear programming framework, each elementary feasible region consists of a polyhedron, and therefore the complete feasible region is a union of polyhedra. While polyhedra are convex, their union does not need to be. In this case, it is impossible to represent such sets using only continuous variables and linear constraints, since this always result in a convex set. Let $\{P_i\}_{i\in I}$ be a finite family of polyhedra, where $P_i = \{x \in \mathbb{R}^n \mid A_i x \leq b_i\}$, and let P be the corresponding union $\bigcup_{i\in I} P_i$. Under certain regularity conditions, we can represent P using the following formula:

$$P = \left\{ x \in \mathbb{R}^n \,\middle|\, \begin{array}{c} A_i x_i \leq z_i b_i,\ \ x = \sum_{x\in I} x_i,\ \sum_{x\in I} z_i = 1\,, \\ x_i \in \mathbb{R}^n,\ z_i \in \{0,1\},\ i \in I \end{array} \right\} \tag{2}$$

The idea of formula (2) is to "activate" a given polyhedron P_i using the corresponding binary variable z_i. Indeed, (2) creates one binary variable z_i and one continuous variable x_i for each polyhedron P_i. It ensures that *exactly* one binary variable is equal to one using the sum-to-one constraint, $\sum_{i\in I} z_i = 1$, and the constraints for x_i are those from the polyhedron P_i, but with right-hand side b_i multiplied by z_i. If the binary variable z_i is equal to one, then x_i belongs to the polyhedron P_i, otherwise the vector x_i satisfies $A_i x_i \leq 0$.

If all polyhedra are bounded, then the only solution to $A_i x_i \leq 0$ is the null vector. Since there is only one j such that $z_j = 1$, the constraint $x = \sum_{i\in I} x_i$ simplifies to $x = x_j$, since all other z_i must be zero, which imply that x_i are equal to the null vector. Therefore, z_j effectively "activated" polyhedron P_j, and all other were "deactivated".

Now, if some of the P_i are unbounded, there are further solutions to $A_i x_i \leq 0$, which are known as *recession directions of* P_i, [5]. Geometrically, such directions are rays such that starting at any point $\overline{x}_i$ in P_i and going indefinitely along x_i we never leave the set P_i:

$$\overline{x}_i + \alpha x_i \in P_i, \quad \text{for every} \quad \alpha \geq 0.$$

We illustrate the use of this formula with the previously presented non-convex operational constraints.

3.1 Binary Minimum Operational Volume

Another possible way of describing the v_{MinOp} rule is by union of polyhedra. Note that Figure 1 is the union of the following sets:

$$\begin{aligned} P_1 &= \{(v_{t+1}, g_t) \mid 0 \leq v_{t+1} \leq v_{\text{MinOp}}, \qquad \underline{G} \leq g_t \leq \overline{g}\} \\ P_2 &= \{(v_{t+1}, g_t) \mid v_{\text{MinOp}} \leq v_{t+1} \leq \overline{v}, \qquad 0 \leq g_t \leq \overline{g}\} \end{aligned}$$

Since P_1 and P_2 are bounded, we can apply the disjunctive constraint formula (2) to describe the desired feasible set using binary variables:

$$P = \left\{ (v_{t+1}, g_t) \;\middle|\; \begin{array}{cc} v_{t+1} = v_{t+1}^1 + v_{t+1}^2 \,, & z_1 + z_2 = 1 \\ g_t = g_t^1 + g_t^2 \,, & z_1,\ z_2 \in \{0,1\} \\ 0 \le v_{t+1}^1 \le z_1 v_{\text{MinOp}} \,, & v_{\text{MinOp}} \le v_{t+1}^2 \le z_2 \overline{v} \\ z_1 \underline{G} \le g_t^1 \le z_1 \overline{g} \,, & 0 \le g_t^2 \le z_2 \overline{g} \end{array} \right\}$$

So, if z_1 is equal to 1, then (v_{t+1}^1, g_t^1) belongs to P_1, z_2 equals 0, and (v_{t+1}^2, g_t^2) is equal to (0, 0). Analogously, if z_2 is equal to 1.

3.2 Binary Minimum Outflow

Let's use the general approach to represent the binary minimum operational feasible set. As can be seen in Figure 2, the union of the following polyhedra describes this set:

$$\begin{aligned} P_1 &= \left\{ (q_t, v_t) \mid v_{\text{crit}} \le v_t \le \overline{v} \,, \quad \underline{q}_1 \le q_t \le \overline{q} \right\}, \\ P_2 &= \left\{ (q_t, v_t) \mid \underline{q}_2 \le v_t \le v_{\text{crit}} \,, \quad q_t \le \underline{q}_2 \right\}, \\ P_3 &= \left\{ (q_t, v_t) \mid 0 \le v_t \le \underline{q}_2 \,, \quad \underline{q}_2 - v_t = 0 \right\}. \end{aligned}$$

Again, all polyhedra are bounded, so the disjunctive constraint theory guarantees that formula 2 describes exactly the union $P = P_1 \cup P_2 \cup P_3$:

$$P = \left\{ (q_t, v_t) \;\middle|\; \begin{array}{ccc} q_t = q_t^1 + q_t^2 + q_t^3 \,, & & z_1 + z_2 + z_3 = 1 \\ v_t = v_t^1 + v_t^2 + v_t^3 \,, & & z_i \in \{0,1\}, i = 1,2,3, \\ z_1 v_{\text{crit}} \le v_t^1 \le z_1 \overline{v} \,, & z_2 \underline{q}_2 \le v_t^2 \le z_2 v_{\text{crit}} \,, & 0 \le v_t^3 \le z_3 \underline{q}_2 \,, \\ z_1 \underline{q}_1 \le q_t^1 \le z_1 \overline{q} \,, & q_t^2 = z_2 \underline{q}_2 \,, & q_t^3 - v_t^3 = 0 \end{array} \right\}$$

It is instructive to note that the relative dimension of P_1 is two, while the relative dimension of P_2 and P_3 is one. So, the disjunctive constraint theory works for a wide variety of polyhedra.

3.3 Non-representable feasible sets

Despite the flexibility, it is not always possible to model union of polyhedra using the theory of disjunctive constraints if one of the polyhedra is unbounded. In Figure 3(a) below we show an example. Note that P_1 is bounded, but P_2 is not, and the direction of recession of P_2 are the rightward directions. If z_1 equals one, then x_1 belongs to P_1, z_2 equals 0, and x_2 is a direction of recession of P_2, that is, $A_2 x_2 \le 0$. Since the disjunctive constraint formula (2) is defined for the sum $x = x_1 + x_2$, we obtain a larger set Q illustrated in Figure 3(b).

Jeroslow [6] proved that if the formula of disjunctive constraints does not represent a given union of polyhedra then no set of linear constraints involving continuous and binary variables is able to represent it. This is an important theorem, since it presents the limits of using binary variables to model union of polyhedra. A sufficient condition for formula (2) to work properly is that all polyhedra P_i have the same set of recession directions. An elementary proof of the Jeroslow theorem and other results of the disjunctive contraints approach can be found in [7].

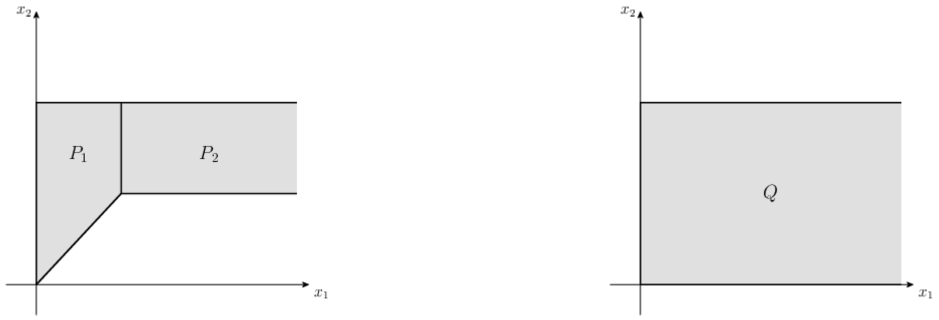

(a) Non-representable feasible set (b) Certificate of non-representability
FIGURE 3: Union of polyhedral non-representable by binary variables and linear constraints

4 Case study: hydrothermal operational planning with disjunctive constraints

In this section, we evaluate the Disjunctive Constraint approach applied to a long-term hydropower system operational planning problem based on the Brazilian Interconnected Power System as of January 2015. The system configuration comprises four interconnected subsystems and the planning period goes from January 2015 to December 2019 considering 60 monthly stages. The minimum operational volume (v_{MinOp}) corresponds to 20% of the maximum storable energy for all months of the planning period. In order to emphasize the effects of the methodologies, we increased the demand by a factor of 5%.

The base case that will be used to evaluate the Binary v_{MinOp} approach is a continuous stochastic optimization problem:

$$Q_t(v_t, \boldsymbol{a}_t) = \min c^\top g_t + c_{df}^\top df_t + \beta \overline{Q}_{t+1}(v_{t+1})$$
$$\text{s.t. } (*)_P$$

$$\overline{Q}_{t+1}(v_{t+1}) = \begin{cases} \rho_t[Q_{t+1}(v_{t+1}, a_{t+1})], & t \in \{1, \dots, T-1\} \\ 0, & t = T \end{cases}$$

where v_{t+1} is the stored energy at the beginning of stage t+1, g_t is the thermal generation during stage t with unit cost $c^\top$, df_t is the deficit (load shedding) during stage t and $c_{df}^\top$ is the corresponding unit cost. The inflow during stage t, $\boldsymbol{a}_t$, is a stagewise independent stochastic process and $(*)_P$ are the physical constraints and other variables. The function $\overline{Q}_{t+1}(v_{t+1})$ is the *future cost-to-go* function, which is an estimator for the future thermal generation and deficit costs of the next stage onward if the storage energy at the end of stage t is v_{t+1}. Such estimator depends on a risk measure ρ_t considered in this case as a convex combination between the expectation and the CVaR: $\rho_t[Z] = (1-\lambda)\mathbb{E}[Z] + \lambda \text{CVaR}_\alpha[Z]$, [8]. We performed all numerical experiments using $\lambda = 0.10$ e $\alpha = 0.05$. Therefore, the objective function minimizes the current cost plus this mean-CVaR estimation of the future cost at each stage. We refer this case as *Base* in the sequel. A more detailed description of these problems can be found in [7].

A usual approach to implement the v_{MinOp} rule is by introducing a penalization in the objective function. We consider a pre-established unit cost $\theta_t^\top$ incurred whenever the stored energy v_{t+1} lies below v_{MinOp}:

$$Q_t(v_t, \boldsymbol{a}_t) = \min_{x_t \in \mathcal{X}_t} c^\top g_t + c_{df}^\top df_t + \beta \overline{Q}_{t+1}(v_{t+1}) + \theta_t^\top (v_{\text{MinOp}} - v_{t+1})_+ \quad (3)$$
$$\text{s.t. } (*)_P,$$

where $(a)_+$ denotes the positive part of number a, i.e., $(a)_+ = \max(0; a)$. We call this problem the Penalty approach. For this study, we consider a penalty value θ_t between the most expensive thermal cost and the cost of the first deficit level so as to ensure all thermal plants units will be dispatched if we fall below v_{MinOp}. In the ensuing text, we refer to this case as *Pen*.

The Binary v_{MinOp} formulation, on the other hand, uses binary variables to dispatch the security thermal units if some coordinate of v_{t+1} is below the corresponding security value v_{MinOp}. We also considered a binary constraint to suppress *preventive* deficit, that is, there is no load curtailment if the stored energy is positive. The corresponding Disjunctive Constraint formulation is

$$\begin{aligned} Q_t(v_t, \boldsymbol{a}_t) = \min_{x_t \in \mathcal{X}_t} \; & c^\top g_t + c_{df}^\top df_t + \beta \overline{Q}_{t+1}(v_{t+1}) \\ \text{s.t. } & (*)_P, \\ & z_d, z_g \in \{0,1\}^{N\text{sys}} \\ & (1 - z_g) v_{\text{MinOp}} \le v_{t+1} \le (1 - z_d)\overline{v}, \\ & MI g_t \ge z_g \underline{G}, \;\; 0 \le df_t \le z_d d_t \end{aligned}$$

where Nsys is the total of subsystems, z_g is the binary vector with value 1 whenever the stored energy of the corresponding subsystem is below the reference volume and zero if not; z_d is the binary vector with component equal to 1 if the corresponding subsystem stored energy is zero. $\overline{v}$ is the maximum stored energy capacity, d_t is the energy demand for time t, $\underline{G}$ is the vector of security thermal dispatch for each subsystem, MI is a 0-1 matrix that links each component of g_t to its subsystem so that MIg_t is the susbsystem thermal generation. Note that the vector product $a\ b$ is a term-by-term product. This will be denoted as *DC* as a reference to the Disjunctive Constraint methodology

4.1 Computational results

The SDDP algorithm, developed for the continuous convex case [9], is the standard method to solve large scale multistage stochastic linear problems like the *Base* and *Pen* cases. Due to the use of binary variables, the *DC* formulation results in non-convex multistage stochastic mixed integer linear optimization problem (MSIP). Recently, these problems became computationally tractable thanks to the development of the SDDiP algorithm [10] that extends the original SDDP algorithm to the class of MSIP problems. However, the SDDiP algorithm requires that the state variables have bounded magnitude, so we had to simplify the scenario generation model to consider stagewise independent historical inflows from 1931 to 2015.

The computational implementation is written in Julia [11], using SDDP.jl [12] and SDDiP.jl [13] open packages and the optimization solver Gurobi v7.0.2 [14]. In the following experiments, we run the algorithm for 1000 iterations with 1 trial solution per iteration and a scenario tree with 85 realizations in every stage resulting in a total number of $1 \times 85 \times \ldots \times 85 = 85^{59}$ scenarios. The individual stage costs and policy value are evaluated using 2000 randomly generated scenarios.

Figure 4 shows the stored energy, deficit, thermal generation and operational costs for each of the policies, considering the first 36 months in order to avoid end of horizon effects. For clarity of visualization, we present only 200 random scenarios in these graphs. In blue, we highlight the decisions of each policy for the same inflow scenario. The first row shows the stored energy values where the red dashed line is the minimum operational energy (v_{MinOp}) along the stages. We can see in Figure 4(a) that some energy stored values for the *Base* policy are below v_{MinOp}. This is expected, since there is no provision in the *Base* (pure CVaR) policy to directly avoid low volumes. The *DC* policy, Figure 4(b), shows small impact on the number of series with stored values below v_{MinOp}. Note that, in contrast with the *Base* policy, the simulated blue series in the *DC* case is above v_{MinOp} in stages 15 and 33 due to the additional thermal generation induced by the binary constraints. On the other hand, *Pen* policy works effectively in terms of increasing the stored volume at each stage: most of the simulated series remain above v_{MinOp} Figure 4(c). However, this policy has a side effect on the deficit variable, as we can see in the following row.

Indeed, both the *Base* and the *DC* policies resulted in low values of deficit, as we observe in Table 1. In Figures 4(d) and 4(e) we can see that almost none of the 200 series resulted in deficit. However, the *Pen* case, Figure 4(f), produces deficit with high frequency, and for the highlighted series, deficit occurs only for the *Pen* case at stage 21, although there still remains resources to meet the demand. The thermal generation policy presents different behavior according to each proposal. In Figure 4(g) we have the *Base* case and when comparing with Figure 4(h) we observe a slight increase in thermal generation in general, where we highlight the security thermal dispatch $\underline{G}$ around stages 8 to 12, 18 to 24 and 32 to 35 induced by the binary constraints. The *Pen* case of Figure 4(i) produces even more thermal generation and the reason is the increase in the future cost induced by the penalty $\theta_t^{\top}(v_{\text{MinOp}} - v_{t+1})_+$. In the series highlighted in blue we see in Figure 4(g) that thermal generation remains below the maximum capacity for all stages in particular also when the storage v_{t+1} is below v_{MinOp}. On the other hand, the case with *DC*, Figure 4(h), thermal generation is at its maximum in all storage occurrences below v_{MinOp} and in *Pen* case, Figure 4(i), thermal generation is close to the maximum throughout the period. We observe that in stage 21 the thermal generation is at the maximum value, which is consistent with the occurrence of a preventive deficit at the stage and case.

The operation cost along the stages is the sum of the cost of thermal generation and the deficit. The operation cost of the *Base* case of Figure 4(j) is low, with few occurrences of costs peaks, since for these 200 simulated series the deficit is very small. In the *DC* case there is also low occurrence of deficit, so the operating cost of Figure 4(k) also presents low occurrence of costs peaks. Additionally, we observe cost boosts associated with thermal generation boosts induced by the binary variable. Figure 4(l) of the *Pen* case presents a higher average cost due to higher thermal generation and higher occurrence of high costs peaks due to greater occurrence of deficit. Note that in each of the operation cost panels, the blue curve accompanies the corresponding movement of the total thermal generation and deficit blue curves.

Although the scenario graph provides a good qualitative idea of the magnitude of interest, it is not an effective plot of the probability density of the simulated quantity along the stages. For this purpose, the violin plot is more appropriate as it is a boxplot-like graph, but uses a method of density estimation at each stage. In order to obtain a more accurate estimation, we evaluated each of the policies in 2,000 historical inflow scenarios to produce the thermal generation violin plots of Figure 5. These graphs comprise only the first 12 stages of simulation. Note that the thermal generation in the *Base* case shown in Figure 5(a) has two points of higher density: the values of 7800 and 9200 MWmonth. The *DC* case of Figure 5(b) has a similar behavior as the *Base* until stage 8, but from stage 9 to stage 12 we have a higher generation in a group of scenarios because of the binary variables. In this case, we also see two points of greater density: the value of 7800 and 11000 MWmonth. In the *Pen* case, Figure 5(c), we clearly see the displaced distribution upwards, with many scenarios between 9000 and 11000 MWmonth.

Finally, we present a quantitative analysis of the deficit for each of the policies evaluated also with 2,000 historical scenarios. Table 1 shows the total deficit added along the 36 simulation stages and over the 2,000 simulated series. Note that for the first deficit level, the *DC* halved the amount of deficit produced in the Southeast relative to the *Base* whereas the *Pen* case multiplied by 10 the deficit in relation to the *Base*. Figure 5 presents a barplot using the first deficit level for each subsystem and policy to emphasize the difference between the magnitudes of deficit. It is worth mentioning that in Table 1 all the levels and subsystems of the *Pen* method results in a deficit amount greater than that of the *Base* case. All the levels and subsystem of the *DC* method have a lower value than the *Base*, except the fourth level of the South where the opposite occurred. Although the number of deficit occurrence in the fourth level is not sufficient for definitive assertions, we have the intuition that the binary constraint that suppress the preventive deficit can have a side effect of producing deficits with larger magnitudes when they occur.

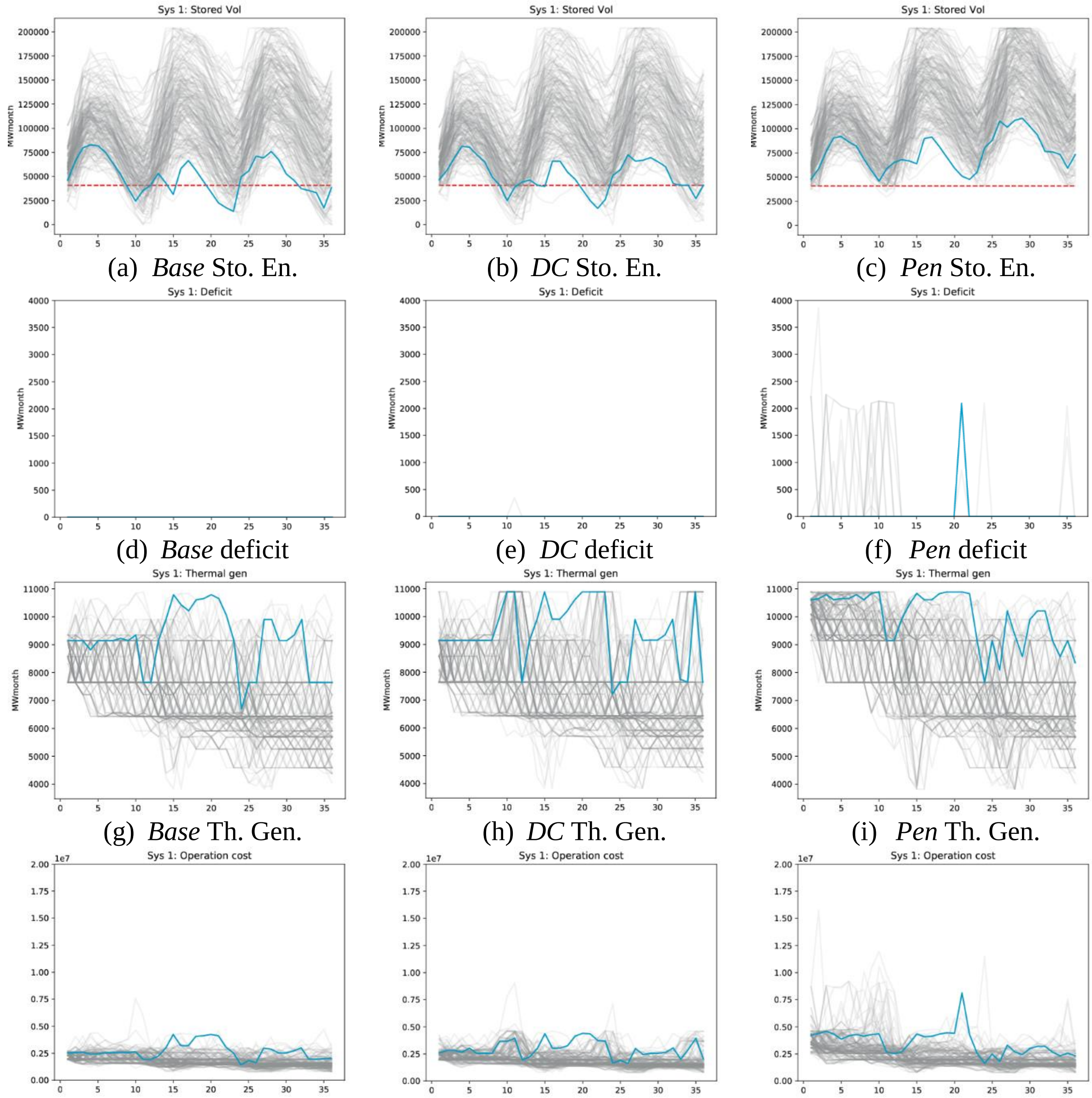

(a) *Base* Sto. En. (b) *DC* Sto. En. (c) *Pen* Sto. En.

(d) *Base* deficit (e) *DC* deficit (f) *Pen* deficit

(g) *Base* Th. Gen. (h) *DC* Th. Gen. (i) *Pen* Th. Gen.

(j) *Base* Op. Cost (k) *DC* Op. Cost (l) *Pen* Op. Cost

FIGURE 4: Stored energy (Sto. En.), deficit, thermal generation (Th. Gen), operational cost (Op. Cost) of pure CVaR (*Base*), CVaR with disjunctive constraints (*DC*) and CVaR with penalization (*Pen*)

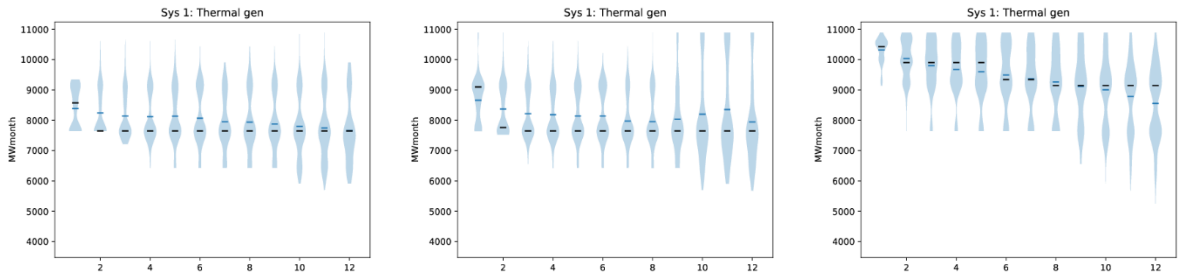

(a) Base *(b) DC* *(c) Pen*

FIGURE 5: Violin plot for thermal generation in the 12 first stages (MWmonth)

TABLE 1: Deficit – *Base*, *DC* and *Pen* (GWmonth).

	Base				*DC*				*Pen*			
Deficit Level	1	2	3	4	1	2	3	4	1	2	3	4
SE	140.5	18.5	9.8	0.0	59.3	15.7	14.4	0.0	1553.6	58.4	0.0	0.0
S	82.8	12.3	5.4	0.0	26.7	7.1	3.5	2.0	468.4	17.5	0.0	0.0
NE	1.4	0.0	0.0	0.0	0.0	0.0	0.0	0.0	9.1	0.0	0.0	0.0
N	1.3	0.2	0.0	0.0	0.6	0.0	0.0	0.0	7.2	0.0	0.0	0.0

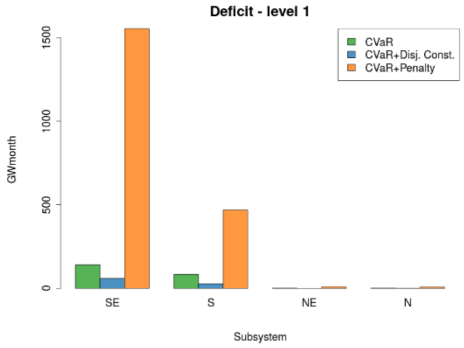

FIGURE 6: First level deficit (GWmonth).

5 Conclusion

In this paper we have presented a general methodology called Disjunctive Constraints for modeling "if-then" nonconvex constraints. In particular, this technique provides a simple and algorithmic way to describe operational constraints using binary variables. Jeroslow proves that the disjunctive constraint technique is the most general framework for modeling non-convex sets by means of linear constraints with binary and continuous variables.

We illustrate the use of this modelling technique with the minimum operational volume and the minimum operational outflow rules for the Brazilian operational planning models. We also analysed an application of this methodology to a large-scale multistage stochastic programming problem, where we have compared the resulting policy with the one obtained by the *Base* model (pure CVaR) and the traditional penalty model for the minimum operational volume rule.

Our results have shown that the Disjunctive Constraint approach performs better than the penalty and the *Base* case, since it precisely models the operational rules and does not produce preventive deficit as a collateral effect of penalties. The use of binary variables in a large-scale multistage stochastic optimization problem was made possible by the SDDiP algorithm.

A future work is to study ways to overcome such modeling limitation imposed by the state variable boundness requirement of the SDDiP algorithm.

BIBLIOGRAPHY

[1] National Water Agency - Brazil, Resolution no 2081 of December 4th, 2017. http://arquivos.ana.gov.br/resolucoes/2017/2081-2017.pdf.
[2] E. Balas, "Disjunctive programming", Annals of Discrete Mathematics, Elsevier, 1979, pp. 3-51.
[3] E. Balas, "Disjunctive programming: Properties of the convex hull of feasible points", Discrete Applied Mathematics, December 1998.

[4] E. Balas, “Disjunctive programming”, In 50 Years of Integer Programming 1958-2008 - From the Early Years to the State-of-the-Art, Springer, 2010, pp. 283–340.
[5] D. P. Bertsekas, Convex Optimization Theory, 1st edition, Athena Scientific, 2009.
[6] R. G. Jeroslow. “Representability in mixed integer programming, I: Characterization results”, Discrete Applied Mathematics, June 1987.
[7] F.G. Cabral, “The role of extreme points for convex hull operations”, MSc dissertation, Applied Mathematics, IMUFRJ, 2018.
[8] A. Shapiro A, W. Tekaya, J.P. Costa, and M.P. Soares, “Risk neutral and risk averse stochastic dual dynamic programming method.” Eur. J. Oper. Res., (2013), 224:375–391.
[9] M. V. Pereira and L. M. Pinto, "Multi-stage stochastic optimization applied to energy planning", Mathematical Programming 52, 1991 pp. 359-375.
[10] J. Zou, S. Ahmed, and A. Sun, "Stochastic dual dynamic integer programming", Optimization Online, 2016, http://www.optimization-online.org/DB_FILE/2016/05/5436.pdf.
[11] J. Bezanson, A. Edelman, S. Karpinski and V.B. Shah, “Julia: A Fresh Approach to Numerical Computing.” (2017) *SIAM Review*, 59: 65–98. doi: 10.1137/141000671. url: http://julialang.org/publications/julia-fresh-approach-BEKS.pdf.
[12] O. Dowson and L. Kapelevich, “SDDP.jl: A Julia package for Stochastic Dual Dynamic Programming”, Optimization Online, 2017, http://www.optimization-online.org/DB_HTML/-2017/12/6388.html
[13] L. Kapelevich, SDDiP.jl: SDDP extension for integer local or state variables, GitHub, 2018, https://github.com/lkapelevich/SDDiP.jl
[14] Gurobi Optimization Inc., Gurobi optimizer reference manual, 2016, http://www.gurobi.com

ACKNOWLEDGEMENT
This work was carried out under contract between UFRJ and ONS, which is greatly acknowledged by the authors.

Biographies

Filipe Goulart Cabral (Rio de Janeiro, RJ, Brazil, 1990) has a B.Sc. in Applied Mathematics (UFRJ, 2013), M.Sc. in Mechanical Engineering (COPPE/UFRJ, 2016) and M.Sc. in Applied Mathematics (IM/UFRJ, Brazil, 2018). Since 2015, he works for ONS, the Brazilian ISO, where he develops methodologies in operations research and statistics applied to power system planning models.

Bernardo Freitas Paulo da Costa (Rio de Janeiro, RJ, Brazil, 1985) has a B.Sc in Engineering (École Polytechnique, France, 2007) and in Applied Mathematics (UFRJ, Brazil, 2009), M.Sc in Mathematics (École Polytechnique and Paris-Sud, 2009) and D.Sc in Mathematics (Paris-Sud, 2012). He has spent a year at Purdue University (2012-2013) as Visiting Assistant Professor, and since 2013 is Professor at UFRJ in the Applied Mathematics department, teaching courses from complex analysis to mathematical optimization, in both graduate and undergraduate levels. Since 2017, he started a technical cooperation with ONS to develop methodologies for non-convex optimization problems in the Energy sector. Bernardo has authored and co-authored papers in complex analysis, optimization and stochastic processes.

Joari Paulo da Costa (Curitiba, PR, Brazil, 1953) has a B.Sc. in Civil Engineering (UFPR, 1976) and Mathematics (PUC-PR, 1976), M.Sc. in Civil Engineering (COPPE/UFRJ, 1982) and D.Sc. in Energy Planning (COPPE/UFRJ, 2007). Since 2000, he is with ONS, the Brazilian ISO, where he is a project manager in the areas of hydrology, optimization and statistical techniques applied to power systems planning and operations. From 1980 to 2000 he has been with Cepel, the Brazilian electric power research center, where he coordinated the development of methodology and software in the above mentioned areas. He has authored and co-authored about forty technical papers in refereed journals and conference proceedings.